

Sequential Decoding of Convolutional Codes with Universal Metric over Bursty-Noise Channel

Byunghyun Moon* · Chaewook Lee*

Abstract

The Fano metric is the maximum likelihood decoding choice for convolutional code for binary symmetric channel. The Fano metric assumes that it has previous knowledge of channel error probability. However, the bit errors in real channel occur in bursts and the channel error probability can not be known exactly. Thus, the Fano metric is not the maximum likelihood choice for bursty-noise channel.

In this paper universal metric which does not require the previous knowledge of the channel transition probability is used for sequential decoding. It is shown that the complexity of the universal is much less than that of the Fano metric bursty-noise channel. since it is estimated on a branch by branch basis

I. Introduction

Since the complexity of the Viterbi algorithm is an exponential function of the code's memory, a sequential decoder is desirable for long constraint length codes and channel memory. To apply the sequential algorithm, a branch metric computed for each branch and the branch with the largest metric is added to the path at the node. Different versions of the sequential algorithm such as the stack algorithm or Fano algorithm can be applied to the decoding tree, as long as the metric

is defined.

Massey (1972) proved that the heuristic Fano metric is actually a logistic choice for maximum likelihood decoding for convolutional codes. However, the Fano metric requires true channel transition probability to calculate the metric.

In this paper, Fano algorithm is used to compare the decoding complexity of the Fano metric and the universal metric over the bursty-noise channel. The effectiveness of the universal metric is shown by computer simulations. Two cases of bursty-noise channel models are considered in the simulation.

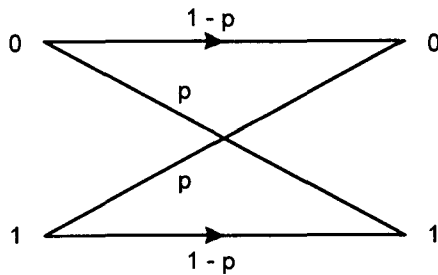
* School of Computer and Communication, Taegu University

** This research was supported by the Taegu University Research Grant, 1997

II. Preliminaries

1. Bursty-noise channel

A discrete communication channel shown in Figure 1 is called a binary symmetric channel (BSC). If the channel input is 0, the channel output is 0 with probability $(1-p)$



<Figure 1> Binary Symmetric Channel

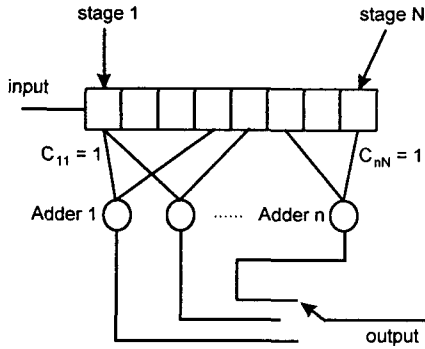
and is 1 with probability p . If the channel input is 1, the channel output is 1 with probability $(1-p)$ and is 0 with probability p . However, the bit errors on real channels occur in bursts which are not well modeled by a memoryless statistical model. Error bursts can occur in military environments (Ziemer and Peterson, 1985), satellite systems (McKenzie, Choi and Braun, 1982), concatenated coding schemes (Wu, Haccoun, Peile and Hirata, 1987; Kaplan, 1990), and from optical storage media such as compact discs (Sklar, 1988).

Channels exhibiting error bursts have been modeled by Markov processes, by impulse noise, and by bursty-noise. For simplicity the bursty-noise in this paper is defined to be the background Gaussian noise plus burst noise, which burst noise is defined to be a series of finite-duration Gaussian noise pulses with variable duration and arbitrary occurrence time.

2. Convolutional Encoder

For the use of BSC, convolutional codes can be generated by a convolutional encoder as shown in Figure 2. The encoder consists of an N bit shift registers and n modulo-2 adders. The connection between a shift register and a modulo-2 adder is specified by a set of coefficients C_{ij} where $i=1,2,\dots,N$ and $j=1,2,\dots,n$. If the i th stage of a shift register is connected to a j th modulo 2 adder, then $C_{ij}=1$. When there is no connection $C_{ij}=0$.

The operation of a convolutional encoder is as follows. Assume that the input $\vec{x}_i = (x_1^i, x_2^i, \dots, x_n^i)$ is to be encoded. First, the contents of all N stages of the shift register are set to zero. Then, the first digit, x_1^i , of \vec{x}_i is shifted into the first stage of the shift registers. The n modulo-2 adders



<Figure 2> Binary Convolutional Encoder

are sampled and passed to the input of the BSC for transmission. This procedure continues until the last component of \vec{x}_i shifts into the first stage of the shift registers.

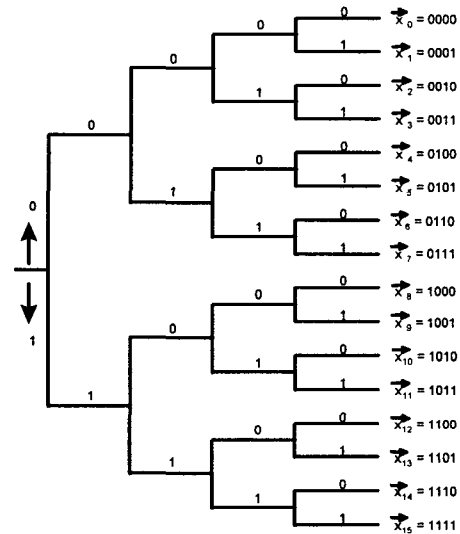
In a shift register encoder, an (n, k) convolutional code is equivalent to k information bits entering the encoder generating n encoded bits. The number N is defined as constraint length of the encoder. Also, the rate of a binary (n, k) convolutional code, R , is defined as

$$R = \frac{k}{n}. \quad (1)$$

3. Tree Structure

This section considers how a convolutional encoder constructs an output

sequence \vec{y} from the input $\vec{x}_i = (x_1^i, x_2^i, \dots, x_n^i)$. The first n digits of \vec{y} are obtained by shifting the first bit x_1^i into the shift register and sampling n modulo-2 adders. An *input tree* can be obtained by adapting the convention that it corresponds to an upward branch if "0" shifts into the shift register and a downward branch if "1" shifts into the shift register. As an example, the set of 16 input sequences with 4 digits long is diagrammed in Figure 3.

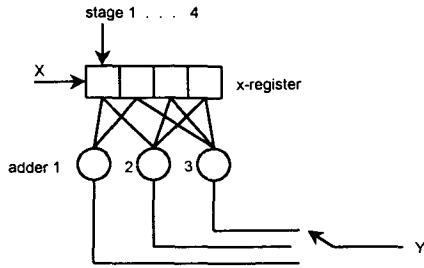


<Figure 3> A set of 16 input sequences \vec{x}_i diagrammed on an input tree.

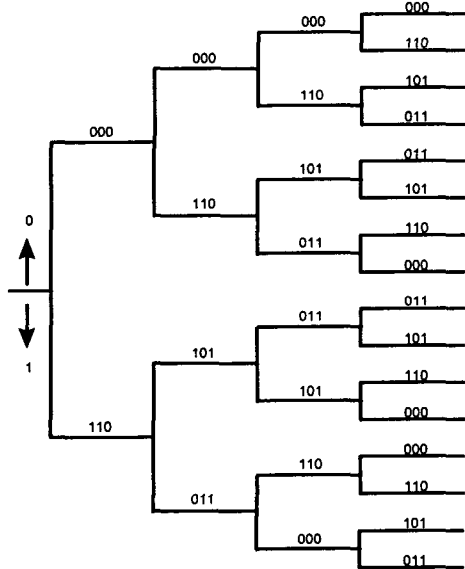
A *code tree* can be obtained by writing along each branch of the input tree the n digits of \vec{y} associated with input sequence.

Consider a particular conventional encoder with $N=4$, $n=3$ and $k=1$ as shown in Figure 4. Then, the corresponding code tree can be constructed as shown in Figure 5. If $k=2$, 4 branches will grow out of a node. In general, 2^k branches will grow out of

a node if k information bits shift into a convolutional encoder. (Zierner and Peterson, 1985)



<Figure 4> Convolutional encoder with $N=4$, $n=3$ and $k=1$.



<Figure 5> Code tree for encoder of Fig. 4.

Define an encoder matrix to be G . Then, the encoder matrix corresponds to Figure 4 can be represented by using the notation C_{ij} introduced previously. An encoder matrix for the encoder shown in Figure 4 is given by

$$G = \begin{bmatrix} C_{11} & C_{12} & C_{13} & C_{14} \\ C_{21} & C_{22} & C_{23} & C_{24} \\ C_{31} & C_{32} & C_{33} & C_{34} \end{bmatrix} = \begin{bmatrix} 1 & 1 & 0 & 0 \\ 1 & 0 & 1 & 1 \\ 0 & 1 & 1 & 1 \end{bmatrix}$$

III. The Universal and Fano Metric

Let Y and Z be two finite sets where $Y=\{0,1\}$ and $Z=\{0,1\}$. Let $\vec{y}=(y_1, y_2, \dots, y_n)$ and $\vec{z}=(z_1, z_2, \dots, z_n)$ be arbitrary n sequences over Y and Z , respectively. Then, the universal metric between \vec{y} and \vec{z} is defined by

$$\Gamma(\vec{y}; \vec{z}) = I(\vec{y}; \vec{z}) - B \quad (2)$$

where B is bias term and $I(\vec{y}; \vec{z})$ is mutual information between \vec{y} and \vec{z} . The mutual information is given by

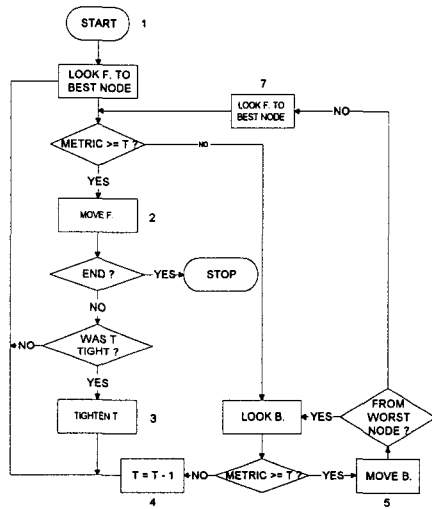
$$\sum_{i=0}^1 \sum_{j=0}^1 p_{\vec{y}\vec{z}}(i, j) \cdot \log \left(\frac{p_{\vec{y}\vec{z}}(i, j)}{p_{\vec{y}}(i) \cdot p_{\vec{z}}(j)} \right) \quad (3)$$

where $p_{yz}(i, j)$ is the probability that $y_n = i$ and $z_n = j$, $p_y(i)$ is the probability that $y_n = i$ and $p_z(j)$ is the probability that $z_n = j$.

The Fano metric is defined as

$$I_F = \sum_{i=1}^n \left[\log \left(\frac{p(z_i|y_i)}{p(z_i)} \right) - R \right] \quad (4)$$

where $p(y_i|x_i)$ is the channel transition probability and R is the rate of the convolutional code. (Gallager, 1969)



<Figure 6> A flowchart description of the Fano Algorithm.

IV. The Fano Algorithm

The Fano algorithm works as follows. At

every stage, the decoder is located at some node in the code tree. From this node, the decoder looks deeper into the tree. If it finds a node with a metric greater than the threshold, T , then it moves to that node. If not, it will move backward and try to move forward along another branch. The details of the Fano algorithm are given in Figure 6. (McEliece, 1985)

V. Example of the Fano Algorithm Using the Universal Metric

In this section, the Fano algorithm using universal metric is illustrated as an example. Consider a (8,1) convolutional encoder with encoder matrix given in Eq. (5).

Assume the input sequence be $\vec{x} = (1, 1, 0, 1)$. Let the output sequence $\vec{y} = (\vec{y}_1, \vec{y}_2, \vec{y}_3, \vec{y}_4)$. Then the

$$G = \begin{bmatrix} 0 & 0 & 1 & 0 & 1 & 0 & 0 & 1 & 0 \\ 1 & 0 & 1 & 1 & 0 & 1 & 0 & 1 & 1 \\ 0 & 1 & 0 & 1 & 1 & 1 & 0 & 1 & 1 \\ 0 & 0 & 1 & 0 & 0 & 0 & 1 & 0 & 0 \\ 0 & 1 & 1 & 0 & 1 & 0 & 1 & 1 & 0 \\ 1 & 0 & 0 & 1 & 0 & 0 & 0 & 1 & 1 \\ 1 & 0 & 0 & 1 & 1 & 0 & 1 & 1 & 0 \\ 1 & 1 & 1 & 0 & 0 & 0 & 1 & 0 & 1 \end{bmatrix}. \quad (5)$$

first 8 digits of \vec{y} is given as $\vec{y}_1 =$

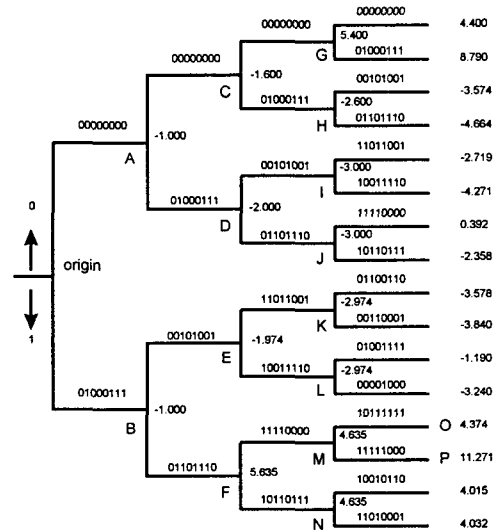
$(0,1,0,0,0,1,1,1)$ corresponding to the first input. Similarly, the rest of the output sequence is given by $\vec{y}_2 = (0,1,1,0,1,1,1,0)$, $\vec{y}_3 = (1,1,1,1,0,0,0,0)$ and $\vec{y}_4 = (1,1,1,1,1,0,0,0)$.

Assume the channel noise sequence be $\vec{n} = (\vec{n}_2, \vec{n}_1, \vec{n}_3, \vec{n}_4)$ where $\vec{n}_1 = (1,1,1,1,0,0,0,0)$, $\vec{n}_2 = (0,0,0,0,0,0,0,0)$, $\vec{n}_3 = (1,1,1,1,0,0,0,0)$ and $\vec{n}_4 = (0,0,0,0,0,0,0,0)$. Then, the channel output sequence $\vec{z} = (\vec{z}_1, \vec{z}_2, \vec{z}_3, \vec{z}_4)$ is given as $\vec{z}_1 = (1,0,1,1,0,1,1,1)$, $\vec{z}_2 = (0,1,1,0,1,1,1,0)$, $\vec{z}_3 = (0,0,0,0,0,0,0,0)$, and $\vec{z}_4 =$

$(1,1,1,1,1,0,0,0)$. Now, the code tree with corresponding metric value calculated from universal metric using Eq. (3) is drawn in Figure 7. The bias term, B , is set to the rate of the code which is $1/8$. Table 1 summarizes the behavior of Fano

algorithm by listing each of the changes in either the node visited or the threshold together with the location in the flow chart in Figure 6 where the changes occur.

Let's define the complexity of the algorithm as the number of the nodes visited until the decoder reaches the last level of the code tree. Then, the complexity of the example above is given by 11.



<Figure 7> Code tree with corresponding metric values for the example

<Table 1> Summary of node visited and the value of threshold.

Step	Node	Threshold	Location
1	origin	0.0	1
2	origin	-1.0	4
3	A	-1.0	2
4	origin	-1.0	5
5	origin	-1.0	6
6	B	-1.0	2
7	F	-1.0	2
8	F	-1.0	3
9	F	5.0	4
10	M	4.0	2
11	P	4.0	2
STOP			

V. Simulation Results

In order to compare the complexity of the universal and Fano metric over binary symmetric channel, Monte Carlo simulations are performed. For a given channel error probability, comparisons are made for the complexity of the algorithm that will determine the efficiency of universal metric and the Fano metric. All the simulation results are based on a fixed code rate of 0.1, a fixed constraint length of 20 with variable k . And, the length of the input sequence is fixed at 100.

The summary of the simulation results is shown in Figure 8 and 9. Figure 8 represents the complexity of universal and Fano metric for $k=2$ with variable channel error probability. The complexity of the universal metric is at least twice as large as the Fano metric. In fact, the complexity of the universal metric is almost 5 times than that of the Fano metric for the channel transition probability of 0.18. Figure 9 shows the complexity of universal and Fano metric for $k=3$ with variable channel error probability. The complexity of universal and Fano metric is similar to the case with $k=2$. As the channel error probability increases, the complexity of universal metric increases drastically. On the other hand, the

complexity of the Fano metric increases slowly.

In order to measure the performance of the universal metric and compare with Fano metric over the bursty-noisy channel, the

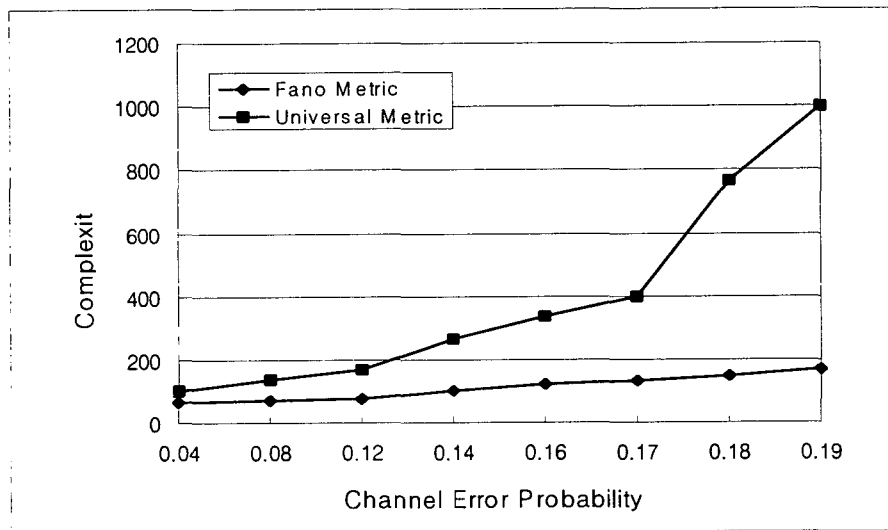
following 2 cases of bursty-noise are considered in the simulations. For case 1, the channel goes into burst error mode with probability 0.1 and the burst noise lasts for 3 branches of code tree with variable channel error probability. For case 2, the channel goes into burst error mode with probability 0.1 and the burst noise lasts for 4 branches of code tree with variable channel error probability. The background channel error probability is deliberately chosen to be low in order to observe the effect of bursty-noise to the metric.

The simulations are based on an input sequence of length 100 with $k=2$ and encoder matrix of 20 by 20. For each case, ten cases of different channel error probability due to background Gaussian noise were tested to compare the complexity of the universal metric with Fano metric over bursty error channel

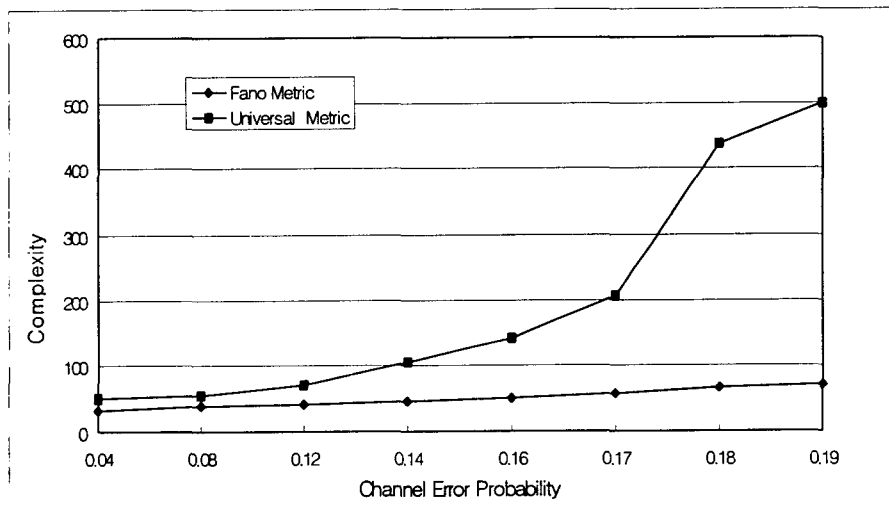
As shown in Figure 10, the complexity of the universal metric over the first case of the bursty-noise is much less than that of Fano metric. As a matter of fact, the complexity of the universal metric is less than half of

the Fano's with the background channel error probability of 0.076. The similar results are obtained for the second bursty-noise as shown in Figure 11. As shown in Figure 10

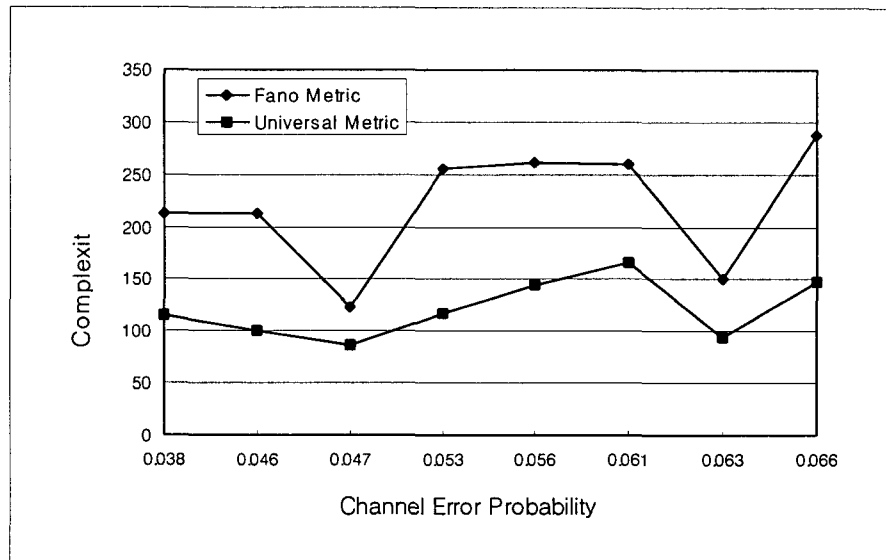
and 11, the complexity of universal metric for the second bursty-noise is slightly higher than the first bursty-noise.



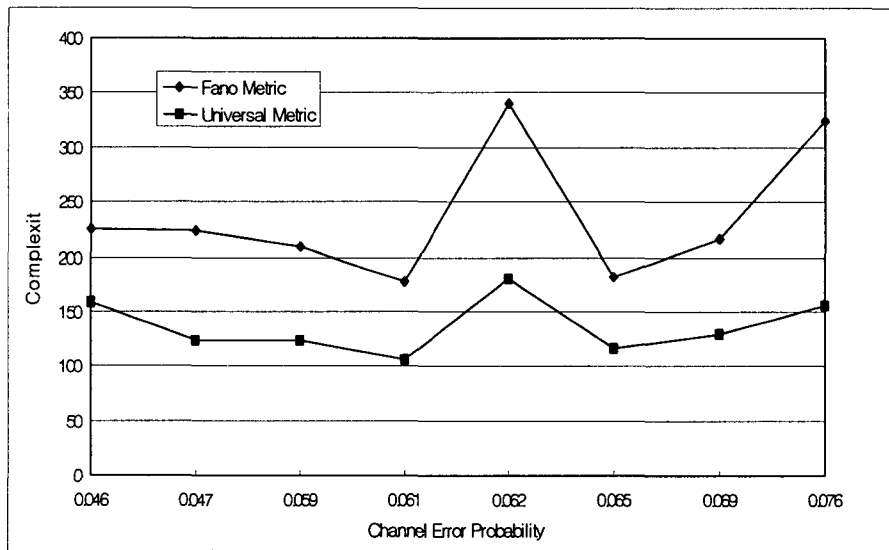
<Figure 8> Complexity of Fano and Universal Metric for k=2.



<Figure 9> Complexity of Fano and Universal Metric for k=3.



<Figure 10> Complexity of Fano and Universal Metric for Bursty-noise Case.



<Figure 11> Complexity of Fano and Universal Metric for Bursty-noise Case 2.

VII. Conclusion

Universal metric that does not require exact channel error probability is proposed for sequential decoding. It is shown that the complexity of the universal metric is much larger than the maximum likelihood metric, Fano metric, for binary symmetric channel.

Since the channel error probability of the bursty-noise channel is different from the exact channel error probability, the complexity of the universal metric is less than the Fano metric over the bursty-noise channel. For the bursty-noise channel, the effectiveness of universal metric for the sequential decoding of convolutional codes is verified.

Reference

- J. L. Massey, "Variable-length codes and the Fano metric," *IEEE Trans. on Inform. Theory*, Vol IT-18, No. 1, pp. 196-198, Jan. 1972.
- R. E. Ziemer, and R. L. Peterson, *Digital Communications and Spread Spectrum Systems*. Macmillan, New York, 1985.
- T. M. McKenzie, H. Choi, and W. R. Braun, Documentation of CLASS Computer Program for Bit Error Rate with RFI, NASA Goddard Space Flight Center, TR-0883-8214-2, August 1982.
- W. W. Wu, D. Haccoun, R. Peile, and Y. Hirata, "Coding for Satellite Communication", *IEEE Journal on Selected Areas in Communications*, Vol. SAC-5, No. 4, May 1987, pp. 742-748.
- T. Kaplan, Characterization of Burst Statistics at the output of the TDRSS Viterbi Decoder, STEI 003-2TK90/M, May 2, 1990.
- B. Sklar, *Digital Communications Fundamentals and Applications*. Prentice Hall, 1988.
- J. M. Wozencraft and I. M. Jacobs, *Principles of Communication Engineering*. New York, John Wiley & Sons, Inc., 1967.
- R. G. Gallager, *Information Theory and Reliable Communication*, New York; John Wiley & Sons, Inc., 1969.
- R. J. McEliece, *The Theory of Information and Coding*, Cambridge, Cambridge University Press, 1985.